

An interactive code for automatic (h- and p-versions) mesh generation and the solution of one-dimensional Bio-heat Equation

(Submitted : 24.02.2020 ; Accepted : 21.09.2020)

Md. Sadekur Rahman Rani¹, Md. Matiar Rahman², Md. Shajedul Karim^{3*}

¹Research Scholar, ²Associate Professor and ^{3*}Professor and Corresponding author
Department of Mathematics, Shahjalal University of Science and Technology, Sylhet, Bangladesh.
E-mail: ¹sustianroni@gmail.com, ²mmrhmman-mat@sust.edu, ^{*}msk-mat@sust.edu

Abstract

In this study, first, we develop an algorithm for the automatic mesh generation employing the n th order one-dimensional finite elements, preparing the elements data, and forming the element connectivity. Secondly, we modify the techniques for evaluating the integrals needed to compute the components of the element matrices and improve the assembly process to form the global matrices. Then, we develop an interactive computer code incorporating all the algorithms and techniques for obtaining the solution of the one-dimensional Bio-heat equation. The code requires only two basic inputs, the order and the total number of the elements in addition to the endpoints of the domain $[a, b]$ for generating the (h- and p-version) meshes and accomplishing the other necessary computations. Since the Bio-heat equation is in the form of a general second-order ordinary BVP, one can use the code conveniently to compute the solutions of the other boundary value problems by providing the actual coefficients of the differential equations. We extensively investigated the performance of the h- and p-methods by calculating the root-mean squares of the errors of the solutions. Finally, for the clarity and reference, we present the solutions of the Bio-heat equation for the four (h- and p-versions) meshes with the corresponding errors.

Keywords: Mesh generation, FE formulation, Bio-heat, Efficiency and Accuracy

1. Introduction

Generally, the domain of the physical problem is discretized either by using numerous elements of lower-order, i.e. using the h-version mesh, or using a few elements of higher-order, i.e. using the p-version mesh. The h- method of FEM is being used commonly for its simplicity and availability of all the relevant algorithms so needed in the FEM solution procedure. It is well known that the h-method generally requires huge computer memory and more computing time. On the other hand, the p-method utilizes p-version meshes that means the method uses a few elements of higher-order for the desired accuracy of the solution. Consequently, this method requires less computer memory and computing time. However, the p-method necessitates faster algorithms mainly: (1) for automatic mesh generation, (2) to prepare element data and connectivity, (3) for evaluation of integrals to form the element matrices, and (4) to assemble the global matrices for obtaining the solution. It is needless to mention that any development on such stages of the p-method of the FEM solution procedure is known as the fundamental development and such developments are indeed highly anticipated. We wish to note here that the mesh generation for the p-method is the prime task, and this initiates avenues of developments for the other stages of the FEM solution procedure.

Since the automatic mesh generation employing the higher-order elements is much more complicated than the mesh generation employing the linear elements. Hence, almost all the commercial software uses only the linear and quadratic elements for generating the h-version and p-version meshes. In practical situations, to solve the real problems, the meshes are generated and refined repeatedly before the final mesh, which also consists of many linear elements [1,4]. So, the computational effort and the computing time increases eventually for obtaining the desired accuracy of the solutions. Therefore, it is an important task to make a proper balance between the accuracy and efficiency of calculations [2- 4]. Thus, it is now desirable to develop faster algorithms for the p-method of the FEM. In this instance, the development of a general algorithm for generating the p-version meshes is the leading task for developing algorithms of the p-method of the FEM.

Considering the above needs mentioned for the developments, the objectives of the study are to (1) develop a suitable algorithm for automatic mesh generation employing a few numbers of the n th order ($n = 1, 2, 3, 4, \dots$) elements; compute the elements data; and to form the element connectivity, (2) present formulae for computing the components of the element matrices, and (3) improve the assembly process of the element matrices to form the global matrices. As an

integral part and also for the completeness of the development, the study intends further to develop an interactive computer code assimilating all the anticipated developed algorithms, formulae, and techniques for solving the one-dimensional boundary value problems.

Many researchers studied the one-dimensional Bio-heat equation and presented numerical and analytical solutions. The necessities and importance so charted to study the said problem are: (a) different therapeutic treatment requires precise monitoring of bio-heat transfer of human tissues for preserving the healthy tissues near the skin surface from burning or freezing during therapeutic application [5], (b) bioheat transfer is the study of heat transfer in the biological system [5-6], (c) the thermal therapies are based on the heat transfer in biological tissues and the purpose of therapeutic application on the biological body is either raising or lowering the temperature at various points in human tissue [5,7], and (d) the heat transfer is a very important process in living tissues to maintain an almost constant temperature. They have also mentioned clearly that the accurate evaluation of the thermal response of the biological tissues during therapeutic applications is very tough due to the complex mechanisms that maintain the body temperatures such as blood flow and metabolic heat generation. So, an important task is to provide useful data on the thermal analysis of biological tissues to the therapist. Furthermore, complex heating is also encountered in thermal diagnostics [8], thermal control analysis [9-12], thermal parameter estimation [12-17], and in burn injury evaluation [18-22].

The finite element formulation of the one-dimensional Bio-heat equation, the FE models employing only the linear elements, and the respective solutions are given in [5]. Due to [5-22], considering the importance and necessities for calculating the accurate results of the bio-heat equation, we think that the p-method will be the appropriate FEM solution procedure. On the other hand, the one-dimensional bio-heat equation is in the form of a more general second-order one-dimensional boundary value problem encountered in many areas of science and engineering. Hence, we are motivated to present the FEM formulation of the Bio-heat equation in the general form so that one can use the formulation for the other second-order one-dimensional boundary value problems. Also, on the line of the development, we intended to develop an interactive computer code in MATLAB based on the general formulation incorporating the algorithms, formulae, and techniques (as expected to develop for the p-method) for obtaining the numerical solutions of the Bio-heat equation with minimum inputs.

2. Bio-heat (Field) Equation

We wish to present here briefly the well-known one-dimensional Bio-heat equation governed by a second-

order ordinary differential equation for ready reference.

The Pennes bioheat transfer equation [5, 13], popularly known as the Bio-heat equation is expressed as

$$\rho c \frac{\partial T}{\partial t} = k \frac{d^2 T_0(x)}{dx^2} + \omega_b \rho_b C_b [T_a - T_0(x)] + Q_m, \quad 0 \leq x \leq L \quad (1)$$

For steady state problem, temperature T is independent of time (t). So, putting $\frac{\partial T}{\partial t} = 0$,

$$C = \omega_b \rho_b C_b \quad \text{and} \quad q = CT_a + Q_m \quad \text{into the governing Eq. (1), the new equation, i.e., the steady state Bio-heat equation becomes} \\ -\frac{d}{dx} \left(k \frac{dT_0(x)}{dx} \right) + CT_0(x) - q = 0 \quad (2)$$

With boundary conditions:

$$\text{At } x = 0, \quad -k \frac{dT_0(x)}{dx} = h_0 [T_f - T_0(x)] \quad (2a)$$

$$\text{At } x = L, \quad T_0(x) = T_c \quad (2b)$$

It is clear in Eqs. (2a)–(2b) that the suppressible boundary condition is at $x = 0$ and the essential boundary condition at $x = L$.

The constants C and q are assumed constants defined by symbols $\omega_b, \rho_b, C_b, T_a$ and Q_m and hence their values and units are known.

All the constants used in Eqs. (1)–(2) and (2a)–(2b) are relevant with the tissue properties, their symbols together with units and values are found in [5,13]. For the purpose of computation these constants are now summarized in Table-1.

2.1 Finite element formulation of the Bio-heat equation

We present here the Finite Element equations in a general form so that both the h- and p-methods can be applied for obtaining the numerical solutions. For the domain $[0, L]$, and the weight functions W , the weak form of Eq. (2) is

$$\int_0^L k \frac{dT_0(x)}{dx} \frac{dW}{dx} dx - \left[k \frac{dT_0(x)}{dx} W \right]_0^L + \int_0^L c T_0(x) \cdot W dx - \int_0^L q \cdot W dx = 0 \quad (3)$$

Discretizing the domain using the finite number of elements where each element has n number of nodes and n number of shape functions of order n ($=n-1$). If we write the nodal value of the function $T_0(x)$ at node

Table- 1
Constants are used in the Bio-heat equation

| Tissue properties | Symbol | Value | Unit |
|--|------------|--------|-------------------------|
| Thermal conductivity of tissue | k | 0.5 | $Wm^{-1} \circ C^{-1}$ |
| Heat convection coefficient between skin & surrounding | h_0 | 10 | $Wm^{-2} \circ C^{-1}$ |
| Force convection co-efficient | h_f | 100 | $Wm^{-2} \circ C^{-1}$ |
| Surrounding air temperature | T_f | 25 | $\circ C$ |
| The arterial temperature | T_a | 37 | $\circ C$ |
| Body core temperature | T_c | 37 | $\circ C$ |
| Metabolic heat generation | Q_m | 33800 | Wm^{-3} |
| Specific heat of tissue | c | 4200 | $Jkg^{-1} \circ C^{-1}$ |
| Specific heat of blood | c_b | 4200 | $Jkg^{-1} \circ C^{-1}$ |
| Density of tissue | ρ | 1000 | kgm^{-3} |
| Density of blood | ρ_b | 1000 | kgm^{-3} |
| The Blood perfusion | ω_b | 0.0005 | $ml/s/ml$ |
| Calculated constant ($c_b \rho_b \omega_b$) | C | 2100 | |
| Calculated constant ($CT_a + Q_m$) | q | 111500 | |

j ($j = 1, \dots, nde$) by T_j and replace the weight function W (for Galerkin weighted residual technique) by shape functions N_i ($i = 1, \dots, nde$), then for an element $[e]$, the trial solution is given by, $T_0(x) = \sum_{j=1}^{nde} T_j N_j$.

Then, the Eq. (3) reduces to,

$$\sum_{j=1}^{nde} T_j \left\{ \int_{[e]} \left(k \frac{dN_i}{dx} \frac{dN_j}{dx} + c N_i N_j \right) dx \right\} = \int_{[e]} q \cdot N_i dx - \left[-k \frac{dT_0(x)}{dx} \cdot N_i \right]_{[e]} \quad (4)$$

Which is now can be written as in the matrix form: $[K]\{T\} = \{F\} + \{B\}$
 Where the components of element matrices $[K], \{F\}, \{B\}$ are defined by,

$$K_{ij} = \int_{[e]} \left(k \frac{dN_i}{dx} \frac{dN_j}{dx} + c N_i N_j \right) dx$$

for $i, j = 1, 2, \dots, nde$ (4a)

$$F_i = \int_{[e]} q \cdot N_i dx, \text{ for } i = 1, 2, \dots, nde \quad (4b)$$

$$B_i = \left[-k \frac{dT_0(x)}{dx} \cdot N_i \right]_{[e]}, \text{ } i = 1, 2, \dots, nde \quad (4c)$$

If we transform the element $[e]$ of global x -space to element $[-1, 1]$ of local ξ - space by using the linear shape functions, then Eqs. (4a)- (4c) reduce to:

$$K_{ij} = \int_{-1}^1 \left(\frac{2}{l} k \frac{dN_i}{d\xi} \frac{dN_j}{d\xi} + \frac{l}{2} c N_i N_j \right) d\xi,$$

for $i, j = 1, 2, \dots, nde$ (5a)

$$F_i = \int_{-1}^1 \frac{l}{2} q \cdot N_i d\xi, \text{ for } i = 1, 2, \dots, nde \quad (5b)$$

$$B_i = \left[-k \frac{dT_0(x)}{dx} \cdot N_i \right]_{[e]}, \text{ } i, j = 1, 2, \dots, nde \quad (5c)$$

It is clear from Eqs.(5a)- (5c) that the order of symmetric element stiffness matrix $[K]$ is $nde \times nde$ where as other element matrices $\{F\}$ and $\{B\}$ are of order $nde \times 1$. So, one has to evaluate $\left\{ \frac{nde(nde+1)}{2} \right\} + nde + nde = \frac{nde(nde+5)}{2}$ integrals for each of the elements of the mesh.

The problem has a suppressible boundary condition at $x = 0$. So, for element $[e] = [1]$ we have to compute the value of B_i at node $i = 1$ that is B_1 and for the other nodes of the elements the value of $B_i = 0, i = 2, 3, \dots, nde$. Using the values of the constants from the table we easily compute, $B_1 = 250$.

So, now we are required to compute $\frac{nde(nde+3)}{2}$ integrals given in Eqs. (5a)- (5b) to form the element matrices. Furthermore, for each integral, the nodal coordinates are required to determine l . The connectivity of the local and global nodes is required to form the global matrices. To meet such requirements, suitable and faster algorithm for mesh generation is needed.

3. Algorithm for Mesh Generation of One-Dimensional Domain

For known LB (initial point of the domain), UB (terminal point of the domain), the total number elements (ELM) and the order of elements (OD), we present an algorithm in the following for automatic mesh generation, to prepare the element data, and forming their connectivity.

Algorithm:

Step-1: Set $NDE=OD+1$,

TOTALNODE=ELM*OD+1 and CORD [1] =LB

Step 2: Set $INCR=(UB-LB) / TOTALNODE$

Step 3: for J=2 to TOTALNODE

compute $CORD[J]=LB+(J-1)*INCR$

Step 4: Set FLAG=0

Step 5: for I=1 to ELM

Step 6: for J=1 to NDE

REL (I,J)=FLAG+J

FLAG=FLAG+OD

Repeat step 6

Repeat step 5

Step 7: Print REL and CORD array and Draw the mesh of the domain

Note that the above algorithm is a general one, it will generate the h- and p-version meshes depending on the values of OD.

3.1 The output of the algorithm and the workflow of the code

We developed an interactive computer code "function oneDimBioheat" incorporating (1) the above mesh generation algorithm, (2) the formulae to evaluate all the integrals (in Eqs. (5a) -(5b)) in order to form the element matrices, (3) the algorithm to assemble the global matrices, and (4) the technique to solve the global system of equations. We wish to include here only the computer code instead of including the assembly algorithm, integration formulae, and solution techniques.

The fragment of the code based on the (mesh generation) algorithm generates the mesh and provides two matrices, namely REL and CORD. The matrix REL represents the connectivity of the local and global nodes, and the matrix CORD presents all the nodal coordinates of the mesh. The remaining fragments of the code take inputs from REL and CORD, then computes components of element matrices, assembles global matrices, and solutions of the Bio-heat equation.

4. Finite Element models

To test the accuracy and efficiency of the higher-order elements, we have considered many FE models by discretizing the domain with elements of different orders. A few of the meshes so generated by the code are shown below:

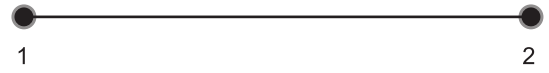
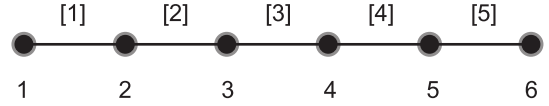
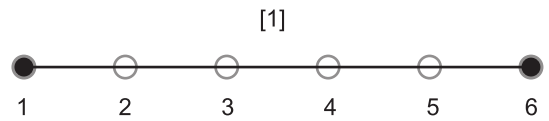


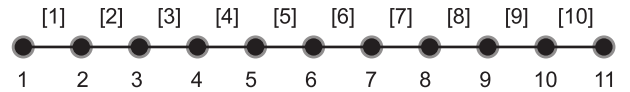
Figure 1: Problem domain, 1 linear element.



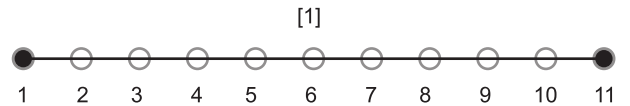
(a) FE Model-1: 5 linear elements mesh



(b) FE Model-2: one 5th order element mesh



(c) FE Model-3: 10 linear elements mesh



(d) FE Model-4: one 10th order element mesh

Figure 2: Domain discretization with (a) five linear elements, (b) one fifth order element, (c) ten linear elements, and (d) one tenth order element.

5.1 Numerical solution of the Bio-heat equation

We mention here that the finite element solution of the Bio-heat equation, Eq. (2) were computed in [5] by using (manually created) h-version meshes. The same equation and the domain are under our consideration for easy comparison of the computed results. To obtain numerical solutions, we used several h- and p-version (code generated) meshes. We computed the percentage of errors for function nodal values to justify the accuracy of the solutions. As only the 4 (four) FE models have shown above, we computed the results and the corresponding percentage of errors. We, for the clear understanding, have summarized them in Tables-(2.1-3.1) and Figs.-(3-4).

Table- 2.1

Comparison of solutions computed by using the FE Model-1 and FE model-2 (both the models have 6 nodes).

| Nodes | FE Model-1(with 5 linear elements) | | FE Model-2(with one 5 th order element) | |
|-------|------------------------------------|---------------------|--|---------------------|
| | App. Solution T _i | Percentage of error | App. Solution T _i | Percentage of error |
| 0 | 43.255588002289123 | 0.14650387486121 | 43.1923099376774 | 0.000000793166909 |
| 0.006 | 44.739782722485828 | 0.15021985586154 | 44.6730827167937 | 0.000911570752205 |
| 0.012 | 44.927973285562977 | 0.14388211463465 | 44.8632132418464 | 0.000467200712201 |
| 0.018 | 43.849349692687227 | 0.12694004093886 | 43.7935278828969 | 0.000525178979513 |
| 0.024 | 41.336607997158943 | 0.08888370749102 | 41.3003224413226 | 0.001025004168894 |
| 0.03 | 37.000000000000000 | 0 | 37 | 0.000000000000000 |
| | $E_{rms} = 1.2 \times 10^{-1}$ | | $E_{rms} = 6.3 \times 10^{-5}$ | |

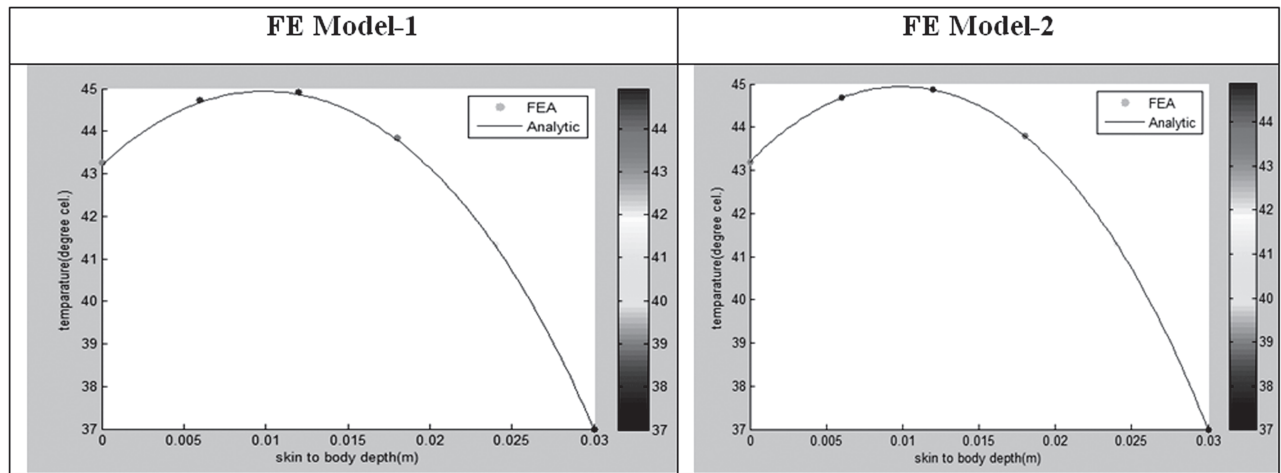


Fig-3: The analytical and numerical solutions for both FE Model-1 and FE model-2

Table-3.1

Comparison of solutions computed by using the FE Model-3 and FE model-4 (both the models have 11 nodes).

| Nodes | FE Model-3(with 10 linear elements) | | FE Model-3(with one 10 th order element) | |
|-------|-------------------------------------|---------------------|---|---------------------|
| | App. Solution T _i | Percentage of error | App. Solution T _i | Percentage of error |
| 0 | 43.20806950875790 | 0.0364877771422 | 43.19230959509 | 0.00000000000921 |
| 0.003 | 44.11942774991822 | 0.0372889529922 | 44.10298220959 | 0.00000000039005 |
| 0.006 | 44.68934930892789 | 0.0373244158626 | 44.67267549378 | 0.00000000073499 |
| 0.009 | 44.93951380230151 | 0.0367785606093 | 44.92299177248 | 0.000000000142748 |
| 0.012 | 44.87943739975789 | 0.0356962413147 | 44.86342284413 | 0.000000000123932 |
| 0.015 | 44.50683481598335 | 0.0339949059752 | 44.49170990104 | 0.00000000018749 |
| 0.018 | 43.80753237917890 | 0.0314531141847 | 43.79375787843 | 0.000000000160576 |
| 0.021 | 42.75492886954860 | 0.0276720433624 | 42.74310098017 | 0.000000000145539 |
| 0.024 | 41.30898361821451 | 0.0219964280158 | 41.29989911560 | 0.000000000063450 |
| 0.027 | 39.41469337419502 | 0.0133627374987 | 39.40942719590 | 0.00000000029821 |
| 0.03 | 37 | 0.0000000000000 | 37 | 0.000000000000000 |
| | $E_{rms} = 3.1 \times 10^{-2}$ | | $E_{rms} = 9.3 \times 10^{-11}$ | |

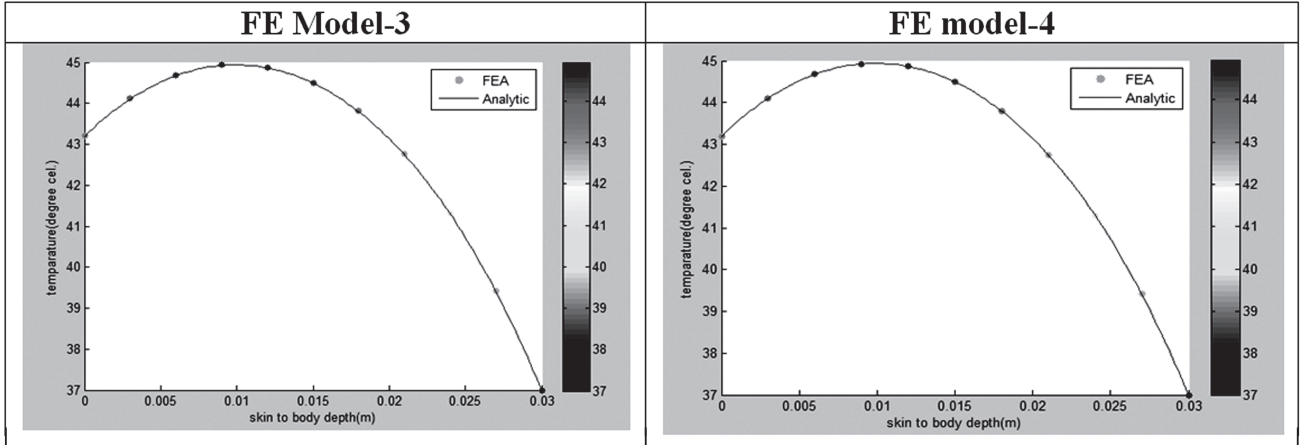


Fig.-4: The analytical and numerical solutions for both FE Model-3 and FE model-4

The analytic solution of the problem

$$T_0(x) = T_a + \frac{Q_m}{\omega_b \rho_b c_b} + \frac{(T_c - T_a - \frac{Q_m}{\omega_b \rho_b c_b})(\sqrt{A} \cosh(\sqrt{A}x) + \frac{h_0}{k} \sinh(\sqrt{A}x))}{\sqrt{A} \cosh(\sqrt{A}L) + \frac{h_0}{k} \sinh(\sqrt{A}L)} + \frac{\frac{h_0}{k}(T_f - T_a - \frac{Q_m}{\omega_b \rho_b c_b}) \sinh(\sqrt{A}(L-x))}{\sqrt{A} \cosh(\sqrt{A}L) + \frac{h_0}{k} \sinh(\sqrt{A}L)}$$

5.2 Performance of h- and p- methods

Numerical solutions for the 4 (four) FE models are shown in Tables-(2.1-3.1). The root-mean square error, E_{rms} is calculated to inspect the performances of the higher-order elements. In Table-2.1, for the FE model-1, the computed $E_{rms} = 1.2 \times 10^{-1}$ whereas the computed $E_{rms} = 6.3 \times 10^{-5}$ for the FE model-2. Which substantiates that we can reduce error 1.9×10^3 times by using one 5th order element instead of using 5 linear elements. Similarly, in Table-3.1 we have $E_{rms} = 3.1 \times 10^{-2}$ for the FE model-3 whereas $E_{rms} = 9.3 \times 10^{-11}$ is found for the FE model-4. Which also substantiates that the accuracy of the solution always higher in case of using the higher-order elements. We have extensively investigated the performance of higher-order elements that is for the p-method considering the h- and p-version meshes. Such results, for clarity and reference are summarized in Table-4.

Table- 4

The requirement of elements for obtaining the solutions correct up to 11 decimal places in different models.

| Order of elements | No. of elements in FE model | E_{rms} |
|-------------------|-----------------------------|-----------------------|
| 10 th | 1 | 9.3×10^{-11} |
| 9 th | 2 | 1.8×10^{-11} |
| 8 th | 3 | 7.2×10^{-12} |
| 7 th | 4 | 5.8×10^{-11} |
| 6 th | 7 | 4.9×10^{-11} |
| 5 th | 15 | 7.5×10^{-11} |
| 4 th | 40 | 7.0×10^{-11} |
| 3 rd | 200 | 6.0×10^{-11} |
| 2 nd | 500 | 4.0×10^{-9} |
| 1 st | 5000 | 1.7×10^{-7} |

Remarks: The computed E_{rms} , in Table-4, clearly shows that the p-method is always efficient in view of the accuracy and efficiency of calculations. Since for example, the p-version mesh consisting of one 10th order (or two 9th order or 200 3rd order) element requires significantly less computer memory and computational effort than that required for the h-version mesh consisting of 5000 linear elements.

6. Conclusions

We have developed an algorithm for automatic mesh generation employing the n -th order one-dimensional finite elements, preparing the elements data, and forming the element connectivity. We have also improved the integration formulae so needed to compute the components of the element matrices and the algorithm to assemble the global matrices. Then, on the line of the development and for the completeness of the objectives, we have developed an interactive (MATLAB) computer code incorporating all the algorithms, formulae, and techniques so needed for the h- and p-methods of the

FEM solution procedure. The workflow of the code is as: (1) it prompts to take the input; the number of elements (NEL); and the order of the elements (OD), (2) it generates the mesh; provides elements data; and the element connectivity, (3) it computes the element matrices, and (4) it assembles the global matrices and computes the solution.

We feel it necessary to mention that the one-dimensional Bio-heat equation is in the general form of the one-dimensional second-order boundary value problems. Many researchers studied the Bio-heat equation and presented analytical/numerical solutions for different situations. They had stressed on the computations of the solutions of the problem with the higher accuracy. So, we have considered the Bio-heat equation as the typical problem for applying the h- and p-methods of the FEM solution procedure. Further, our motive for considering the Bio-heat equation was: (1) the computer code for its solution will be applicable for the other BVPs, (2) the computed results can be easily compared with the solutions available in the literature, and (3) since the length of the domain is practically small; the p-version mesh will be the suitable one to model the problem domain. Thus, we have developed the code "function oneDimBioheat" which is a complete one for obtaining the solutions of the said problem by the h- and p-methods. This code easily may be used for computing the solutions of the other BVPs by providing the domain and the value of the actual coefficients of the differential equations.

We have considered the (manually created h-version) FE models of [5] and generated the same FE models and then computed the corresponding solutions using the code. We have found the full agreement of the meshes and the solutions. Then, by using the code, we have generated other (h- and p-versions) meshes; obtained solutions, and then compared the computed solutions with the existing analytical/ numerical solutions. Such, computed results (for the four FE models) are presented in tabular form and displayed graphically. Further, we have extensively investigated the performances of the higher-order elements in terms of the solution accuracy and efficiency of calculations. In several test cases, by calculating the root-mean squares of the errors, we have substantiated that a vast number of lower-order elements are required in the mesh for the h-method than that of a p-method for obtaining the same accuracy. We are impressed to note here that the use of the higher-order elements drastically reduces the number of elements of the mesh. Consequently, the p-method requires less computer memory and computational effort. This fact is illustrated in Table-4. The agreement of the numerical and analytical solutions ensures the correctness of the mesh generation algorithm, computation of element matrices, and their assembly. We believe that the main

contribution of this study, the algorithm for the automatic (h- and p-versions) mesh generation, will open avenues for developing suitable algorithms to generate the two- and three- dimensional meshes. We anticipate that the ultimate contribution of the study, the computer code, will find immense applications for solving one-dimensional field problems encountered in many areas of science and engineering.

7. Computer Code

```
function oneDimBioheat
format long
syms z
%information for domain
a=0; %lower limit
b=0.03; %upper limit
%Information for elements
elm=input('Number Of Elements:');
order=input('Order Of Elements:');
l=(b-a)/elm; %length of element
%node numbers
nde=order+1;
totalnode=elm*order+1;
%nodal coordinates
x=linspace(0,0.03,totalnode);
%generating shape function
N=oneDShapeFunction(order);
dN=diff(N);
%problem constants (used in FEM formulation)
k=0.5;
c=2100;
q=111500;
% Relations between Global and local nodes
%Domain discretization
flag=0;
for i=1:elm
for j=1:nde
rel(i,j)=flag+j;
end
flag=flag+order;
end
%initiazing the matrices with 0
gk=zeros(totalnode,totalnode)';
gf=zeros(1,totalnode);
gb=zeros(1,totalnode);
%impose suppressible boundary condition
gb(1,1)=250;
%Calaculation K,F, element matrices
m=1;
for e=1:elm
for i=1:nde
fe(i)=int(N(i)*q*1/2,'z',-1,1);
for j=1:nde
ke(i,j)=int(k*dN(i)*dN(j)*2/l+c*N(i)*N(j)*1/2,'z',-1,1);
end
```

```

end
%assemble K,F matrices one by one element
p=1;
for i=1:nde
n=1;
gf(rel(m,p))=gf(rel(m,p))+fe(i);
for j=1:nde
gk(rel(m,p),rel(m,n))=gk(rel(m,p),rel(m,n))+
ke(i,j);
n=n+1;
end
p=p+1;
end
m=m+1;
end

F=gf+gb;
%impose essential at last node of the domain
Tc=input('Essential b.c (temparature at x=L):');
newk=gk(1:totalnode-1,1:totalnode-1);
newf=(F(1:totalnode-1))'-gk(1:totalnode-1,totalnode)*Tc;
newk(1,1)=newk(1,1)+10;

%to solve the global system of equations
t=inv(newk)*newf;
t(totalnode)=Tc;
%displaying the result
disp(x');
disp('app:');
disp(t);
disp('exact:');
exct=exact(x');
disp(exct');
%Error calculation
for i=1:totalnode
err(i)=100*abs(exct(i)-t(i))/abs(exct(i));
end
disp('Error:');
for i=1:totalnode
fprintf('%0.15f\n',err(i));
end
% to display the result in figure
figure;
scatter(x,t,100,t,'filled');
colormap(jet(n));
colorbar;
hold on
%curve of exact solution
xx=linspace(0,0.03,100);
yy=exact(xx');
plot(xx,yy);
xlabel('skin to body depth(cm)');
ylabel('temparature(degree cel.)');
s=0;
nm=size(err,2);

for i=1:nm
s=s+(err(1,i))^2;
end
disp('RMS error:');
disp(double(sqrt(s/nm)));
end
function [s]=oneDShapeFunction(order)
syms z
nde=order+1;
t=2/order;
for i=1:nde
x(i)=-1+(i-1)*t;
end
for i=1:nde
N=1;
for j=1:nde
if i==j
continue;
end
N=N*(z-x(j))/(x(i)-x(j));
end
s(i)=N;
end
end
function [tt]=exact(xx)
[m n]=size(xx);
syms x
format long
k=0.5;
h0=10;
hf=100;
tf=25;
ta=37;
tc=37;
qm=33800;
c=4200;
cb=4200;
p=1000;
pb=1000;
wb=0.0005;
l=0.03;
t=inline(((ta+(qm/(wb*pb*cb)))+((tc-ta-(qm/(wb*pb*cb))))*
(sqrt(wb*pb*cb/k)*cosh(sqrt(wb*pb*cb/k)*x)+(h0/k)*
sinh(sqrt(wb*pb*cb/k)*x))/(sqrt(wb*pb*cb/k)*
cosh(sqrt(wb*pb*cb/k)*1)+(h0/k)*sinh(sqrt(wb*pb*cb/k)*1))))+
((h0/k)*(tf-ta-(qm/(wb*pb*cb))))*(sinh(sqrt(wb*pb*cb/k)*(1-x))/(sqrt(wb*pb*cb/k)*cosh(sqrt(wb*pb*cb/k)*1)+(h0/k)*
sinh(sqrt(wb*pb*cb/k)*1)))));
for i=1:m
tt(i)=t(xx(i));
end
end

```


Acknowledgement

We have accomplished this work under the activities of a SUST Research Center funded project (Project ID: PS/2018/2/18, 2018-2019). We are deeply grateful to the Director and members of the Center and the Authority of Shahjalal University of Science and Technology, Sylhet, Bangladesh.

References

1. Barret, K.E., Explicit Eight-noded Quadrilateral Elements, *Finite Elements in Analysis and Design*. 1999, 31; 209-222.
2. Videla, L. et.al., Explicit Integration of the stiffness Matrix, *AIAAJ*. 1996, 6; 1174-1176.
3. Yagawa, G., Ye, G.W. and Yashimara, S., A Numerical Integration scheme for Finite element Method based on symbolic manipulation, *Int. J. Numer. Method. Engng.* 1990, 29; 153-159.
4. Rathod, H.T. and Karim, M.S., Synthetic division Based Integration of Rational functions of Bivariate Polynomial Numerators over a unit triangle $\{0 \leq s, t \leq 1, s + t \leq 1\}$ in the local parametric space, *Compute. Methods. Appl. Mech. Engng.* 2000, 181; 191-235.
5. Mst. Nasima Bagum and Abul Anam Rashed. Finite Element Analysis of One-Dimensional Bio-Heat Transfer in Human Tissue, *IOSR Journal of Engineering (IOSRJEN)*. 2013, 3(6); 43-49.
Website: http://en.wikipedia.org/wiki/Bioheat_transfer (last modified on 9 April 2011 at 03:33, Retrieved: July,24,2011)
6. Florin, F., Andrei, B. I., Iulia, C. M., Computer-aided analysis of the heat transfer in skin tissue, 3rd WSEAS Int. Conference on finite differences - finite elements - finite volumes - boundary elements, Vol. 53, pp.53-59.
7. Liu, J., Xu, L.X., Boundary Information Based Diagnostics on the Thermal States of Biological Bodies, *Int. J. Heat Mass Transf.* 2000, 43; 2827-2839.
8. Markee, N.L., Hatch, K.L., Maibach, H.I., Barker, R.L., Radhakrishnaiah, P., Woo, S.S., Perceived Sensations to Three Experimental Garments Worn by Subjects Exercising in a Hot, Humid Environment, *Textile Research Journal*. 1990, 60; 561-568.
9. Burch, S.D., Ramadhyani, S., Pearson, J.T., Analysis of Passenger Thermal Comfort in an Automobile under Severe Winter Conditions, *ASHRAE Trans., ASHRAE Winter Meeting, Atlanta*. 1991; 247-257.
10. Arens, E., Bosselmann, P., Wind, Sun and Temperature. Predicting the Thermal Comfort of People in Outdoor Spaces, *Building and Environ.* 1989, 24; 315-320.
11. Chato, J.C., Measurement of Thermal Properties of Growing Tumors, *Ann. N.Y. Acad. Sci.* 1980, 335; 67-85.
12. Pennes, H.H., Analysis of Tissue and Arterial Blood Temperatures in the Resting Human Forearm, *J. Appl. Physiol.* 1948, 1; 93-122.
13. Patera, A.T., Mikic, B.B., Eden, G., Bowman, H.F., Prediction of Tissue Perfusion from Measurement of the Phase Shift Between Heat Flux and Temperature, *Winter Annual Meeting of ASME, Advances in Bioengineering*, 1979; 187-191.
14. Patel, P.A., Valvano, J.W., Pearce, J.A., Prahl, S.A., Denham, C.R., A Self-Heated Thermistor Technique to Measure Effective Thermal Properties from the Tissue Surface, *ASME J. Biomech. Eng.* 1987, 109; 300-315.
15. Anderson, G.T., Valvano, J.W., Santos, R.R., Self-heated Thermistor Measurements of Perfusion, *IEEE Trans. Biomed. Eng.* 1992, 39; 877-885.
16. Liu, J., Xu, L.X., Estimation of Blood Perfusion Using Phase Shift in Temperature Response to Sinusoidal Heating at the Skin Surface, *IEEE Trans. Biomed. Eng.* 1999, 46; 1037-1043.
17. Torvi, D.A., Dale, J.D., A Finite Element Model of Skin Subjected to a Flash Fire, *ASME J. Biomech. Eng.* 1994, 116; 250-255.
18. Diller, K.R., Modeling of Bioheat Transfer Processes at High and Low Temperatures, *Adv. Heat Transfer*. 1992, 22; 157-357.
19. Weinbaum, S., Jiji, L.M., Lemons, D.E., Theory and Experiment for the Effect of Vascular Microstructure on Surface Tissue Heat Transfer-Part I: Anatomical Foundation and Model Conceptualization, *ASME J. Biomech. Eng.* 1984, 106; 321-330.
20. Holmes, K. R., Biological Structures and Heat Transfer, *Allerton Workshop on the Future of Biothermal Engineering*, 1997.
21. Zhong-Shan, D., Jing, L., Analytical study on bio-heat transfer problems with spatial or transient heating on skin surface or inside biological bodies, *Journal of Biomechanical Engineering*. 2002, [DOI: 10.1115/1.1516810].